Universal oscillations in counting statistics

C. Flindt[a,b,1], C. Fricke[c], F. Hohls[c], T. Novotný[b], K. Netočný[d], T. Brandes[e], and R. J. Haug[c]

[a]Department of Physics, Harvard University, 17 Oxford Street, Cambridge, MA 02138; [b]Department of Condensed Matter Physics, Faculty of Mathematics and Physics, Charles University, Ke Karlovu 5, 12116 Prague, Czech Republic; [c]Institut für Festkörperphysik, Leibniz Universität Hannover, D 30167 Hannover, Germany; [d]Institute of Physics, Academy of Sciences of the Czech Republic, Na Slovance 2, 18221 Prague, Czech Republic; and [e]Institut für Theoretische Physik, Technische Universität Berlin, D 10623 Berlin, Germany

Edited by Peter Zoller, University of Innsbruck, Innsbruck, Austria, and approved April 22, 2009 (received for review January 29, 2009)

Noise is a result of stochastic processes that originate from quantum or classical sources. Higher-order cumulants of the probability distribution underlying the stochastic events are believed to contain details that characterize the correlations within a given noise source and its interaction with the environment, but they are often difficult to measure. Here we report measurements of the transient cumulants $\langle\langle n^m \rangle\rangle$ of the number n of passed charges to very high orders (up to $m = 15$) for electron transport through a quantum dot. For large m, the cumulants display striking oscillations as functions of measurement time with magnitudes that grow factorially with m. Using mathematical properties of high-order derivatives in the complex plane we show that the oscillations of the cumulants in fact constitute a universal phenomenon, appearing as functions of almost any parameter, including time in the transient regime. These ubiquitous oscillations and the factorial growth are system-independent and our theory provides a unified interpretation of previous theoretical studies of high-order cumulants as well as our new experimental data.

cumulants | distributions | electron transport | noise and fluctuations

Counting statistics concerns the probability distribution P_n of the number n of random events that occur during a certain time span t. One example is the number of electrons that tunnel through a nanoscopic system (1–4). The first cumulant of the distribution is the mean of n, $\langle\langle n \rangle\rangle = \langle n \rangle$, the second is the variance, $\langle\langle n^2 \rangle\rangle = \langle n^2 \rangle - \langle n \rangle^2$, the third is the skewness, $\langle\langle n^3 \rangle\rangle = \langle (n - \langle n \rangle)^3 \rangle$. With increasing order the cumulants are expected to contain more and more detailed information on the microscopic correlations that determine the stochastic process. In general, the cumulants $\langle\langle n^m \rangle\rangle = S^{(m)}(z = 0)$ are defined as the mth derivative with respect to the counting field z of the cumulant generating function (CGF) $S(z) = \ln \Sigma_n P_n e^{nz}$. Recently, theoretical studies of a number of different systems have found that the high-order cumulants oscillate as functions of certain parameters (5–9), however, no systematic explanation of this phenomenon has so far been given. Examples include oscillations of the high-order cumulants of transport through a Mach-Zender interferometer as functions of the Aharonov-Bohm flux (6), and in transport through a double quantum dot as functions of the energy dealignment between the two quantum dots (8). As we shall demonstrate, oscillations of the high-order cumulants in fact constitute a universal phenomenon which is to be expected in a large class of stochastic processes, independently of the microscopic details. Inspired by recent ideas of M. V. Berry for the behavior of high-order derivates of complex functions (10), we show that the high-order cumulants for a large variety of stochastic processes become oscillatory functions of basically any parameter, including time in the transient regime. We develop the theory underlying this surprising phenomenon and present the first experimental evidence of universal oscillations in the counting statistics of transport through a quantum dot.

We first present our experimental data. In our setup (Fig. 1*A*), single electrons are driven through a quantum dot and counted (11–16), using a quantum point contact. The quantum dot is operated in the Coulomb blockade regime, where only a single additional electron at a time is allowed to enter and leave. A

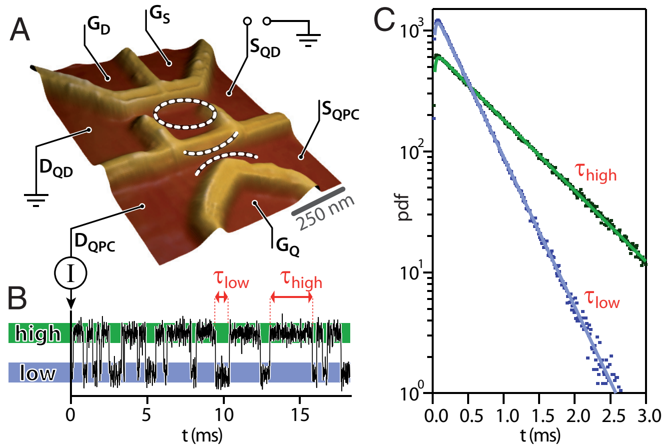

Fig. 1. Real-time counting of electrons tunneling through a quantum dot. (*A*) Atomic force microscope topography of the quantum dot (QD, dashed ring) and the quantum point contact (QPC, dashed lines). The gates G_S and G_D are used to electrostatically control the tunneling barriers between QD and source (S_{QD}) and drain (D_{QD}) electrodes, respectively. The gate G_Q is used to tune the QPC. (*B*) Typical time-trace of the current from S_{QPC} to D_{QPC} via the QPC. The current switches between a high and a low level: as an electron tunnels onto the QD from S_{QD}, the QPC current is suppressed. The suppression is lifted as the electron leaves via D_{QD}. Electrons passing through the QD are counted by monitoring switches of the QPC current. (*C*) Measured (unnormalized) probability density functions (pdf) for the switching times τ_{low} and τ_{high} shown with dots. For short times the data display a kink due to the finite detector bandwidth. The lines show theoretical predictions taking $\Gamma_D = 2.97$ kHz, $\Gamma_S = 1.46$ kHz, and $\Gamma_Q = 40$ kHz as fitting parameters. The asymmetry parameter is $a = -0.34$.

large bias-voltage across the quantum dot ensures that the electron transport is uni-directional. Electrons enter the quantum dot from the source electrode at rate $\Gamma_S = \Gamma$ and leave via the drain electrode with rate $\Gamma_D = \Gamma(1 - a)/(1 + a)$, where $-1 \leq a \leq 1$ is the asymmetry parameter (14, 15). A nearby quantum point contact (QPC) is capacitively coupled to the quantum dot and used as a detector for real-time counting of the number of transferred electrons during transport: When operated at a conductance step edge, the QPC current is highly sensitive to the presence of localized electrons on the dot. By monitoring switches of the current through the QPC (see Fig. 1*B*) it is thus possible to detect single electrons as they tunnel through the quantum dot and thereby obtain the distribution of the number of transferred electrons P_n. In the experiment we fix the asymmetry parameter a and monitor the time evolution of the number of passed charges. This requires a single long time-trace of

Author contributions: C. Flindt, C. Fricke, F.H., T.N., K.N., T.B., and R.J.H. designed research, performed research, and wrote the paper.

The authors declare no conflict of interest.

This article is a PNAS Direct Submission.

[1]To whom correspondence should be addressed. E-mail: flindt@physics.harvard.edu.

This article contains supporting information online at www.pnas.org/cgi/content/full/0901002106/DCSupplemental.

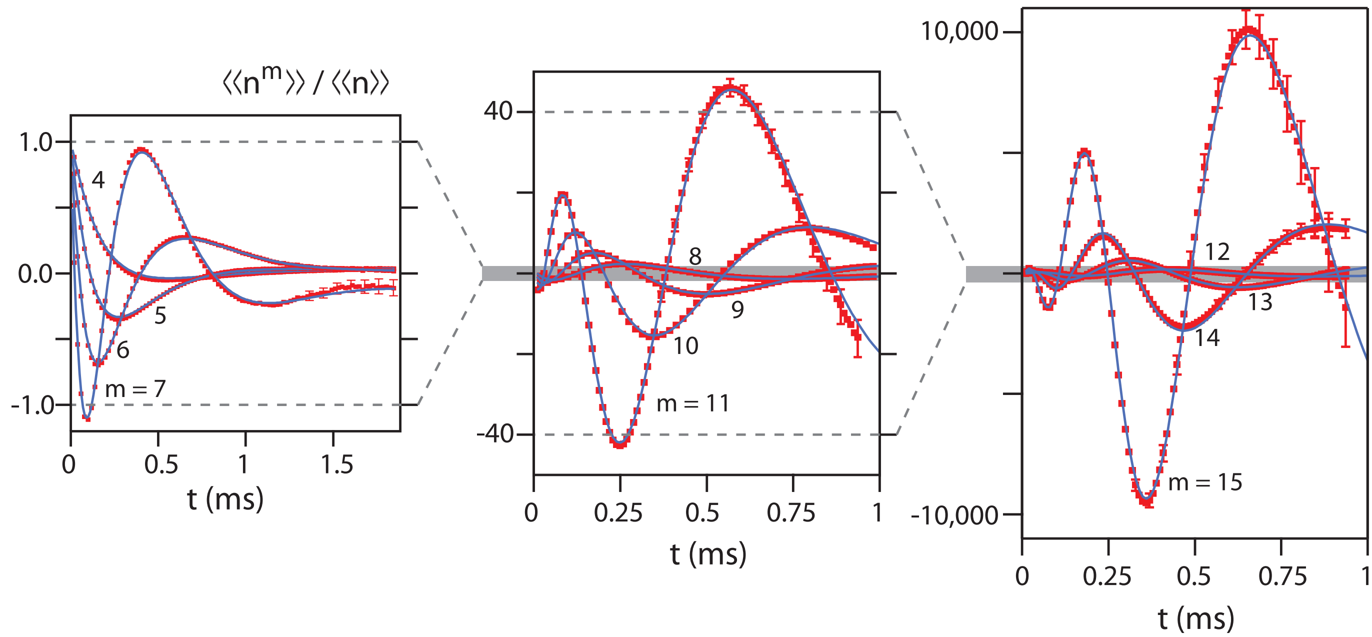

Fig. 2. Measurement of high-order cumulants. Experimental results (squares) for the time evolution of the first 4–15 cumulants. The cumulants clearly show oscillations as functions of time, with increasing magnitude and number of oscillations for higher orders m. The theoretical model (full lines) shows excellent agreement with the experimental data. For very high orders ($m \geq 10$) the finite number of electron counts during the experiment limits the statistical accuracy to times shorter than $\approx$1 ms. The estimates for the error bars are discussed in *Methods*. Parameters corresponding to the data shown here are given in the caption of Fig. 1.

duration T during which a large number of tunneling events are counted. The time-trace is divided into a large number N of time segments of length t. From the number of electrons counted in each time segment we find the probability distribution P_n from which the cumulants as functions of measurement time are obtained. In this approach t can be varied continuously as it was recently shown experimentally up to the fifth cumulant (15). For the experiment considered here $\approx$670,000 electrons were counted during a time span of $T = 770$ s. This allowed us to estimate P_n for t in the range from 0 to $\approx$2 ms. In Fig. 2, we show the corresponding experimental results for the time evolution of the high-order cumulants up to order 15. Most remarkably, the cumulants show transient oscillations as functions of time that get faster and stronger in magnitude with increasing order of the cumulants.

Together with the experimental results, we show theoretical fits of the cumulants as functions of measurement time. The model is based upon a master equation (17) and takes into account the finite bandwidth of the detector (15, 18), which is not capable of resolving very short time intervals between electron tunneling events (see *SI Appendix*). The detector bandwidth Γ_Q and the rates Γ_D and Γ_S are the only input parameters of the model and they can be extracted from the distribution of switching times, shown in Fig. 1*C*, between a high and a low current through the quantum point contact. The calculated cumulants show excellent agreement with the experiment for the first 15 cumulants as seen in Fig. 2.

The master equation calculation per se does not provide any hints concerning the origin and character of the oscillations seen in the experiment. Similarly, in the theoretical studies of high-order cumulants mentioned previously (5–9), no systematic explanation of the origin of these oscillations has been proposed. Here, we point out the universal character of the oscillations of high-order cumulants and develop the underlying theory. The following analysis applies to a large class of stochastic processes, including the aforementioned theoretical studies and the experiment described above. We thus consider a general stochastic process with a CGF denoted by $S(z,\lambda)$. Here, all relevant quantities related to the system—collectively denoted as λ—enter as real parameters. As it follows from complex analysis, the asymptotic behavior of the high-order cumulants is determined by the analytic properties of the CGF in the complex z plane. We consider the generic situation, where the CGF $S(z,\lambda)$ has a number of singularities z_j, $j = 1, 2, 3, \ldots,$ in the complex plane that can be either poles or branch-points. Exceptions to this scenario do exist, e.g., the simple Poisson process, whose CGF is an entire function, i.e., it has no singularities. Such exceptions, however, are nongeneric and are excluded in the following, although they can be addressed by analogous methods (10). Close to a singularity $z \approx z_j$ the CGF takes the form $S(z, \lambda) \approx A_j/(z - z_j)^{\mu_j}$ for some A_j and μ_j. The corresponding derivatives for $z \approx z_j$ are $\partial_z^m S(z, \lambda) \approx (-1)^m A_j B_{m,\mu_j}/(z - z_j)^{m+\mu_j}$ with $B_{m,\mu_j} = (\mu_j + m - 1)(\mu_j + m - 2) \ldots \mu_j$ for $m \geq 1$. The approximation of the derivatives becomes increasingly better away from $z \approx z_j$ as the order m is increased. This is also known as Darboux's theorem (10, 19). For large m, the cumulants are thus well-approximated as a sum of contributions from all singularities,

$$\langle\langle n^m \rangle\rangle \approx \sum_j (-1)^{\mu_j} A_j B_{m,\mu_j} / z_j^{m+\mu_j} \quad [1]$$

This simple result determines the large-order asymptotics of the cumulants. Generally, the singularities come in complex-conjugate pairs, ensuring that the expression above is real. Although actual calculations of the high-order cumulants using this expression may be cumbersome, the general result displays a number of ubiquitous features. In particular, we notice that the magnitude of the cumulants grows factorially with the order m due to the factors B_{m,μ_j}. Furthermore, writing $z_j = |z_j|e^{i\mathrm{Arg}(z_j)}$ with $|z_j|$ being the absolute value of z_j and $\mathrm{Arg}(z_j)$ the corresponding complex argument, we also see that the most significant contributions to the sum come from the singularities closest to $z = 0$. The relative contributions from other singularities are suppressed with the relative distance to $z = 0$ and the order m, such

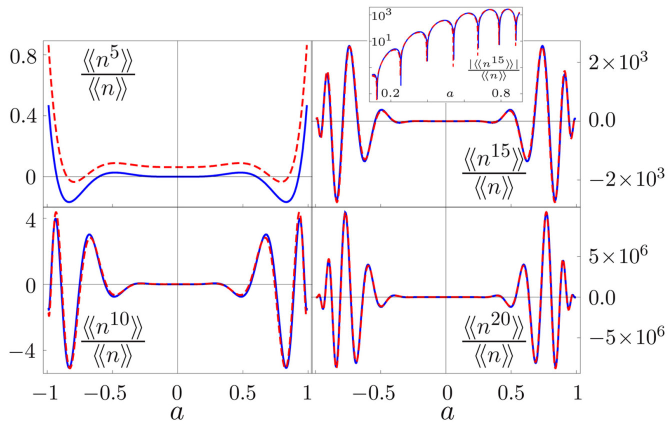

Fig. 3. Universal oscillations of cumulants. High-order cumulants in the long-time limit as functions of the asymmetry parameter *a*. We assume an ideal detector with infinite bandwidth. Full lines correspond to exact theoretical results for the cumulants, while dashed lines show the asymptotic approximation using the two dominating singularities z_0 and z_{-1} closest to $z = 0$ (see Fig. 4*A*). As the order *m* is increased, the asymptotic approximation becomes better, and for $m \geq 10$, the two curves are nearly indistinguishable. The cumulants are clearly oscillatory functions of the asymmetry parameter. As the order is increased, the number and amplitudes of the oscillations grow. The inset shows the absolute value of the 15th cumulant on a logarithmic scale for $0.1<a<0.9$.

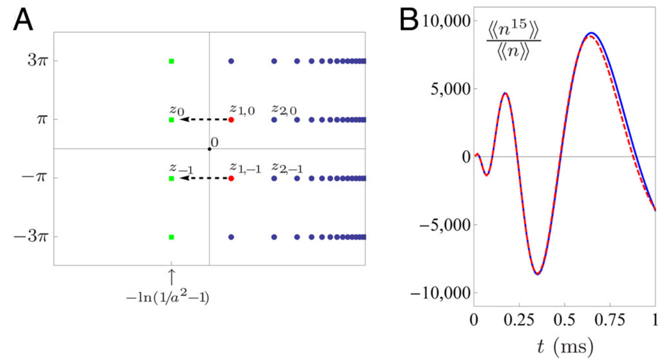

Fig. 4. Singularities in the complex plane and universal oscillations as function of measurement time. (*A*) Complex plane with the singularities of the CGF. The singularities $z_j = -\ln(1/a^2 - 1) + (2j + 1)i\pi$, $j = \ldots -1,0,1,\ldots$, corresponding to the linear-in-time term of the CGF are shown with green squares. Among these singularities, z_0 and z_{-1} are closest to $z = 0$ and thus responsible for the oscillations of the cumulants in the long-time limit seen in Fig. 3. The time-dependent singularities $z_{k,j}$, $k = 1,2,\ldots$, $j = \ldots -1,0,1,\ldots$, are shown with colored circles. The arrows indicate the motion with time of the two dominating singularities $z_{1,-1}$ and $z_{1,0}$ (shown with red). Here, parameters are $a = -0.34$, $t = 0.3$ ms, and $\Gamma_Q \to \infty$. (*B*) Transient oscillations of the 15th cumulant as function of time with $a = -0.34$ and $\Gamma_Q \to \infty$. The full line corresponds to exact theoretical results, whereas the dashed line shows the asymptotic approximation using the dominating singularities $z_{1,-1}$ and $z_{1,0}$. For $t \geq 0.6$ ms, a slight deviation is seen. We attribute this to the singularites $z_{2,-1}$ and $z_{2,0}$, which also come close to 0. The curves agree well with the experimental results in Fig. 2, even if the finite-bandwidth of the detector has not been included here.

that they can be neglected for large *m*. Most importantly, we recognize that the high-order cumulants become oscillatory functions of any parameter among λ that changes $\mathrm{Arg}(z_j)$ as well as of the cumulant order *m*. This important observation shows that the high-order cumulants for a large class of CGFs will oscillate as functions of almost any parameter.

For a simple illustration of these concepts, we consider a charge transfer process described by a CGF reading

$$S(z,\lambda) = \frac{\Gamma t}{1+a}(w_{z,a} - 1) + \ln\frac{1 + q_{z,a}e^{-2w_{z,a}\Gamma t/(1+a)}}{1 + q_{z,a}} \qquad [2]$$

with $w_{z,a} \equiv \sqrt{(1-a^2)e^z + a^2}$, $q_{z,a} \equiv -(1-w_{z,a})^2/(1+w_{z,a})^2$ and $\lambda = \{t,a,\Gamma\}$. This would correspond to our experiment in the case of an ideal detector with infinite bandwidth ($\Gamma_Q \to \infty$) (see *SI Appendix*). Let us start by analyzing the first, linear-in-time term of the CGF which corresponds to the long-time limit. This term has branch points at $z_j = -\ln(1/a^2 - 1) + (2j+1)i\pi$, $j = \ldots -1,0,1,\ldots$, for which the argument of the square-root entering the definition of $w_{z,a}$ is zero. Parameters corresponding to these singularities are $A_j = i\Gamma t|a|/(1+a)$ and $\mu_j = -1/2$. Clearly, the positions of these singularities vary as the asymmetry parameter is changed, which modifies the complex argument $\mathrm{Arg}(z_j)$, and we thus expect oscillations of the high-order cumulants in the long-time limit as functions of the asymmetry parameter *a*. In Fig. 3 we show the approximation for the cumulants obtained by including in the sum only the contributions from the singularities z_0 and z_{-1} that are closest to $z = 0$. The approximation is compared with exact calculations of the cumulants obtained by direct differentiation of the CGF in the long-time limit and shows nearly perfect agreement for large orders. The fifth cumulant in the long-time limit has already been measured as a function of the asymmetry parameter, showing some indication of the onset of these oscillations (15).

Finally, we now return to our experimental data presented in Fig. 2. In the transient regime we see that the high-order cumulants oscillate as functions of measurement time. This is due to the time dependence of the dominating singularities of the CGF. In the case of an ideal detector ($\Gamma_Q \to \infty$) (see *SI Appendix*) the CGF at finite times in Eq. **2** has time-dependent singularities when the argument of the logarithm is zero. These singularities have the form $z_{k,j} = x_k + (2j+1)i\pi$, $k = 1,2,\ldots$, $j = \ldots -1,0,1,\ldots$, where $x_k \equiv \ln\lfloor(a^2 + u_k^2)/(1-a^2)\rfloor$ and u_k solves the transcendental equation $2u_k\Gamma t/(1+a) - 4\arctan(1/u_k) = 2\pi(k-1)$ (see Fig. 4*A*). The derivatives of the logarithmic singularity encountered here can be treated with our theory by formally setting $\mu_{k,j} = 0$ and $\mu_{k,j}A_{k,j} = 1$. In Fig. 4*B* we see that the approximation for the 15th cumulant as function of time, using the two time-dependent singularities $z_{1,-1}$ and $z_{1,0}$ closest to $z = 0$ for the given time interval, agrees well with exact calculations in the limit of an ideal detector ($\Gamma_Q \to \infty$), taking $a = -0.34$ as in the experiment. The curves are also in good agreement with the experimental results in Fig. 2, showing that the oscillations cannot be dismissed as an experimental artifact due to, e.g., the finite bandwidth of the detector. Of course, in the long-time limit the cumulants relax to their linear-in-time asymptotics given by the first term of the CGF. The low-order cumulants ($m = 4-7$) seen in Fig. 2, normalized with respect to the first cumulant, clearly reach their long-time limits for $t \geq 1.5$ ms. This does not contradict the fact that the cumulants oscillate as functions of time in a given finite time interval for high enough order.

The experimental and theoretical results presented in this work clearly demonstrate the universal character of the oscillations of high-order cumulants. In our experiment the high-order cumulants oscillate as functions of time in the transient regime. As our theory shows, such oscillations are however predicted to occur as functions of almost any parameter in a wide range of stochastic processes, regardless of the involved microscopic mechanisms. The universality of the oscillations stems from general mathematical properties of cumulant generating functions: as some parameter is varied, dominating singularities move in the complex plane, causing the oscillations. Oscillations of high-order cumulants have been seen also in other branches of physics, including quantum optics (20) and elementary particle physics (21), further demonstrating the universality of the phenomenon.

Methods

Device. The quantum dot and the quantum point contact were fabricated using local anodic oxidation techniques with an atomic force microscope on the surface of a GaAs/AlGaAs heterostructure with electron density $n = 4.6 \times 10^{15} m^{-2}$ and mobility $\mu = 64 m^2/Vs$. With this technique the 2-dimensional electron gas residing 34 nm below the heterostructure surface is depleted underneath the oxidized lines on the surface. A number of in-plane gates were also defined, allowing for electrostatic tuning of the quantum point contact and electrostatic control of the tunneling barriers between the quantum dot and the source and drain electrodes.

Measurement. The experiment was performed at an electron temperature of about 380 mK, as determined from the width of thermally broadened Coulomb blockade resonances. To avoid tunneling from the drain to the source contact of the quantum dot due to thermal fluctuations, we applied a bias of 330 μV across the quantum dot. The QPC detector was tuned to the edge of the first conduction step. The current through the QPC was measured with a sampling frequency of 100 kHz. This sufficiently exceeded the bandwidth of our experimental setup of about 40 kHz. The tunneling events were extracted from the QPC signal using a step detection algorithm.

Error Estimates. To estimate the error of the experimentally determined cumulants we created an ensemble of simulated data using the same rates as observed in the experiment. We then extracted the cumulants for each simulated data set in the ensemble and determined the ensemble variance of the cumulants for each order m as function of time t. The error bars in Fig. 2 show the square-root of the variance.

ACKNOWLEDGMENTS. We thank N. Ubbelohde (Hannover, Germany) for his support in the development of the data analysis algorithms, W. Wegscheider (Regensburg, Germany) for providing the wafer, and B. Harke (Hannover, Germany) for fabricating the device. The work was supported by the Villum Kann Rasmussen Foundation (C. Flindt), the Czech Science Foundation Grant 202/07/J051 (to C. Flindt, T.N., and K.N.), Federal Ministry of Education and Research of Germany via nanoQuit (C. Fricke, F.H., and R.J.H.), German Excellence Initiative via the "Centre for Quantum Engineering and Space-Time Research" (C. Fricke, F.H., and R.J.H.), research plan MSN0021620834 financed by the Ministry of Education of the Czech Republic (to T.N.), project AV0Z10100520 in the Academy of Sciences of the Czech Republic (to K.N.), and Deutsche Forschungsgemeinschaft Project BR 1528/5–1 (to T.B.).

1. Blanter, Ya M, Büttiker M (2000) Shot noise in mesoscopic conductors. *Phys Rep* 336:1.
2. Nazarov YV, ed (2003) *Quantum Noise in Mesoscopic Physics* (Kluwer, Dordrecht, The Netherlands).
3. Levitov LS, Lesovik GB (1993) Charge-distribution in quantum shot-noise, *JETP Lett* 58:230.
4. Levitov LS, Lee H, Lesovik GB (1996) Electron counting statistics and coherent states of electric current. *J Math Phys* 37:4845.
5. Pilgram S, Büttiker M (2003) Statistics of charge fluctuations in chaotic cavities. *Phys Rev B* 67:235308.
6. Förster H, Pilgram S, Büttiker M (2005) Decoherence and full counting statistics in a Mach-Zehnder interferometer. *Phys Rev B* 72:075301.
7. Förster H, Samuelsson P, Pilgram S, Büttiker M (2007) Voltage and dephasing probes in mesoscopic conductors: A study of full-counting statistics. *Phys Rev B* 75:035340.
8. Flindt C, Novotný T, Braggio A, Sassetti M, Jauho A-P (2008) Counting statistics of non-Markovian quantum stochastic processes. *Phys Rev Lett* 100:150601.
9. Novaes M (2008) Statistics of quantum transport in chaotic cavities with broken time-reversal. *Phys Rev B* 78:035337.
10. Berry MV (2008) Universal oscillations of high derivatives. *Proc R Soc London Ser A* 461:1735.
11. Lu W, Ji ZQ, Pfeiffer L, West KW, Rimberg AJ (2003) Real-time detection of electron tunnelling in a quantum dot. *Nature* 423:422.
12. Bylander J, Duty T, Delsing P (2005) Current measurement by real-time counting of single electrons. *Nature* 434:361.
13. Fujisawa T, Hayashi T, Tomita R, Hirayama Y (2006) Bidirectional counting of single electrons. *Science* 312:1634.
14. Gustavsson S, et al. (2006) Counting statistics of single-electron transport in a quantum dot. *Phys Rev Lett* 96:076605.
15. Gustavsson S, et al. (2007) Measurements of higher order noise correlations in a quantum dot with a finite bandwidth detector. *Phys Rev B* 75:075314.
16. Fricke C, Hohls F, Wegscheider W, Haug RJ (2007) Bimodal counting statistics in single-electron tunneling through a quantum dot. *Phys Rev B* 76:155307.
17. Andrews GE, Askey R, Roy R (1999) *Special Functions* (Cambridge Univ Press, Cambridge), Sec 6.6.
18. Bagrets DA, Nazarov, Yu V (2003) Full counting statistics of charge transfer in Coulomb blockade systems. *Phys Rev B* 67:085316.
19. Naaman O, Aumentado J (2006) Poisson transition rates from time-domain measurements with a finite bandwidth. *Phys Rev Lett* 96:100201.
20. Dodonov VV, Dremin IM, Polynkin PG, Man'ko VI (1994) Strong oscillations of cumulants of photon distribution function in slightly squeezed states. *Phys Lett A* 193:209.
21. Dremin IM, Hwa RC (1994) Quark and gluon jets in QCD—factorial and cumulant moments. *Phys Rev D* 49:5805.